GeoConvention 2015
GEOSCIENCE
new horizons
Telus Convention Centre • 4-8 May 2015 • Calgary, AB Canada

Influence of Shale Anisotropy on Caprock Stress Determination

Jeremy Gallop
Ikon Science Canada Ltd.

Summary

The calculation of caprock shale stress is important to maintain isolation between reservoir and overburden, as well as optimize reservoir completions and operating strategies. Continuous profiles of stress can be calculated from well logs, but this requires some approximation to determine the full set of transverse anisotropic parameters required in this process. In this study we model shales of varying silt content with and without horizontal cracks to understand the impact of a particular anisotropic approximation. It is found that the ANNIE approximation ($\delta = 0$ and $c_{12} = c_{13}$) works well except when horizontal cracks are present, in which case it overestimates the overburden contribution to the horizontal stresses.

Introduction

Caprock shales play an important role in isolating hydrocarbon reservoirs from overburden fresh water aquifers. This is especially important for reservoirs subjected to thermal recovery such as those in the McMurray Formation (Collins, 2002). Minimum in-situ stress is an important parameter to quantify in caprocks, as it affects the ability of a shale to contain fractures generated beneath during thermal operations (Smith et. al. 2001). Parallel considerations exist in shale reservoir exploitation, where well completions need to be optimized and fracture containment within a zone is desirable (Higgins et. al. 2008). Determination of in-situ stresses are best carried out by minifrac estimates but suffer the drawback of only sampling discrete depths within a borehole. Well logs have been used to predict continuous vertical profiles of stress using both isotropic and anisotropic formulations (Thiercelin and Plumb, 1994), that latter being superior if anisotropic data are available (Waters et. al. 2011). The accuracy of the continuous stress profile is limited by the assumption of linear poroelasticity, the ability of logs to produce the full suite of elastic moduli (Sayers 2010) and finally the empirical nature of dynamic to static calibrations (Holt et. al., 2013). Rock physics modelling can provide insight into the stress calibration process, and provide scenarios to understand how geologic and structural parameters should influence the accuracy of the results. Anisotropic shale modelling was pioneered by Hornby et.al. (1994) and has seen recent widespread application in gas and kerogen-rich shales (e.g. Ren and Spikes, 2014). One drawback of the method is the large number of parameters that need to be measured from core, inferred from log fit or simply assumed. More recently Ortega (2009) has suggested possible simplifications based on observations of shale behaviour at high clay packing density; the essence of the method has also been adapted by Pervukhina et. al. (2015). These models are based on solid shales without cracks, the source of their anisotropy being the fabric of the material; cracks can be added as a final step as necessary. In this study we shall use a modified form of the Ortegan model to study the effect of silt inclusions, porosity and cracks parallel to bedding on the estimation of stress in shale formations. The latter is a realistic concern, given that erosion and glacial retreat can remove overburden, creating an unloaded stress path. Figure 1 shows the plausibility of such cracks in an example of a shallow caprock in NE Alberta.

Theory

The shale models of Ortega et. al. (2009) are based on a 3 tiered approach. In level zero, a compacted pure clay is assumed with zero porosity, VTI symmetry and elastic moduli

$c_{11} = 44.9, c_{13} = 18.1, c_{12} = 21.7, c_{33} = 24.2, c_{44} = 3.7, c_{66} = 11.6$, where all units are in GPa. These constants have been deduced from regressions on a variety of data. This is a unique aspect of their findings: the moduli are independent of specific clay type. In level 1, microporosity is embedded in the solid clay using spherical inclusions and the self-consistent approximation (SCA) specifically to preserve the percolation behaviour at $\kappa \approx 50\%$ where κ is the wet clay porosity defined by $\kappa = \phi/(1-f_s)$, and f_s is the silt fraction in the shale. The percolation threshold is fixed in Ortega et. al. (2009), however this study uses the naturally occurring SCA threshold closer to 55% porosity as seen in Figure 5 of Hornby et. al. (1994). At level 2 the host is embedded with silt inclusions (again spherical) within the SCA framework, and as a final step we optionally include fluid filled cracks, with low aspect ratio. Four our calculations, the SCA representation has incorporated VTI anisotropy and ellipsoidal inclusions, the details for which the reader is referred to Hornby et. al. (1994), Nishizawa (1982), and Jakobsen et. al. (2003). We note that the SCA approach treats fluids as isolated inclusions. This assumption is a matter of debate in the rock physics community, where it is uncertain if a passing wave could potentially have pressures equalize between some cracks and pores and not others (Xu and Payne, 2009).

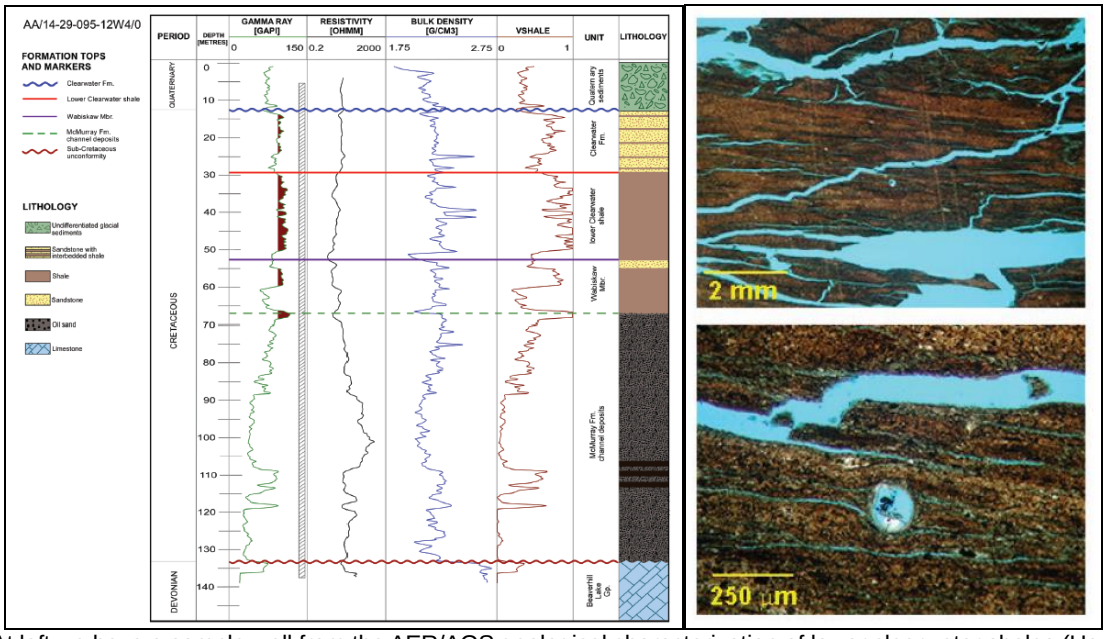

Figure 1: At left we have a sample well from the AER/AGS geological characterization of lower clearwater shales (Haug et. al. 2014). At right are thin section photomicrographs from 35m depth; the fractures highlighted in blue are attributed to coring, pressure release and sample dessication but also indicate that microcracks parallel to bedding possibly exist insitu.

The properties modelled thus far are dynamic and correspond to seismic wave velocities. However, static properties characterized by larger strains and drained conditions are needed to calculate stresses. To calibrate dynamic to static properties the relationship used for Young's Modulus is applied in an anisotropic sense, and is shown below:

$$E_{ii}^{stat} = a(E_{ii}^{dyn})^b + c. \quad (1)$$

where the subscript runs from 1 to 3 (no summation implied) and all units are in GPa. The Poisson's ratios (vertical and horizontal) were not scaled, like Higgins et. al. (2008), and the constants used above are a=0.032, b=1.72, and c=1.0. The equations of linear poroelasticity are used to predict in-situ stresses from log measurements (Thiercelin and Plumb, 1994). In this analysis a VTI medium is assumed with equal horizontal stresses, leading to a horizontal in-situ stress composed of two terms:

$$\sigma_h - \alpha_h P_p = K_0(\sigma_z - \alpha_v P_p) + K_1 \varepsilon_h \quad (2)$$

where $\sigma_h(\sigma_v)$ are the horizontal (vertical) stresses, P_p is the pore pressure, ε_h is the lateral strain and α_h, α_v are the Biot-Willis coefficients, set to unity in our calculations. Estimates of pore pressure can be made from hydrostatic curves while overburden stress is integrated from from density logs. The constants K_0 and K_1 are what we desire to know from measured logs and are often calibrated to geomechanical core tests. They can be written:

$$K_0 = \frac{c_{13}}{c_{33}} = \frac{[\sqrt{2c_{33}(c_{33}-c_{44})\delta + (c_{33}-c_{44})^2} - c_{44}]}{c_{33}} \quad (3)$$

$$K_1 = \frac{1}{s_{11}+s_{12}} = 2[c_{33}(1+2\varepsilon) - c_{44}(1+2\gamma)] - 2\frac{[\sqrt{2c_{33}(c_{33}-c_{44})\delta + (c_{33}-c_{44})^2} - c_{44}]^2}{c_{33}} \quad (4)$$

where the notation is more compact using Voigt stiffness (c_{ij}) or compliances (s_{ij}), but are shown in the more familiar $\varepsilon, \delta, \gamma$ parameters of Thomsen (1986) along with the moduli c_{33} and c_{44}, which correspond to vertically travelling P- and S-wave velocities, respectively. The two terms on the right hand side of equation (2) can be interpreted as overburden and tectonic terms respectively, the latter requiring knowledge of an assumed constant lateral strain existing in all formations. We see that the Vp/Vs ratio and δ control the overburden term and a combination of $\varepsilon, \delta, \gamma, c_{33}$ and c_{44} control the tectonic term. It is generally assumed that the tectonic term is important in areas of with significant compression and hence lateral strain, while the overburden term is dominant in areas with little tectonic stress. However, it should be noted that even regions remote from tectonic activity, plastic strains are formed in the 1D compaction of shales internally (Katahara, 2009) and opposing elastic strains are generated which contribute to the tectonic term in equation (2). The static data set required for the stress calculation above is $\{c_{11}^{stat}, c_{12}^{stat}, c_{13}^{stat}, c_{33}^{stat}\}$; these can be found using equation (1) from their corresponding dynamic values, which are approximated from the log data set $\{c_{33}^{dyn}, c_{44}^{dyn}, c_{66}^{dyn}\}$; the static values $c_{44}^{stat}, c_{66}^{stat}$ are not required. Some examination of Thomsen's parameters will show that δ and ε are not measured by logs. The ANNIE approximation of Schoenberg et.al. (1996) is a common way to circumvent this problem by assuming that $\delta = 0$ and $c_{12} = c_{13}$. It can be shown that this leads to the relationship $\varepsilon = 2c_{44}\gamma / c_{33}$, thus providing constraint on the missing δ and ε parameters. This is often a reasonable approach, but we shall conduct some modeling to show where discrepancy may arise.

Results

Below we carry out the SCA shale model using isotropic silt grains composed of a Voigt-Reuss-Hill average of 10% calcite, 20% feldspar and 70% quartz, with bulk and shear moduli of K=40.1GPa and G=33.9GPa. The brine bulk modulus is 2.16GPa. Figure 2 (left) show the P- and S-wave velocities and Thomsen's parameters as a function of porosity and silt content for in-tact shale. Anisotropy is seen to increase as porosity decreases, whereas it tends to decrease with elevated silt content. Values for δ are in the range –0.05 to 0.05, which is small compared to existing core studies. When cracks parallel to bedding are introduced in Figure 2 (right) with a crack density of 0.12 and an aspect ratio of 1.e-3, we see a decrease in bedding perpendicular velocities, an increase in γ, and δ now becomes negative. This effect has been noted before by Vernik and Liu (1997) for fluid saturated cracks. The stress coefficients K_0 and K_1 are shown for the same models in Figure 3. The dashed red lines are the ANNIE approximations to the grey calculated stress coefficients, with the same light to dark colour scheme. We can see that in the unfractured case (left side of Figure 3), the overburden coefficient K_0 increases with higher clay content (less silt), a well known result. The tectonic coefficient K_1 displays the opposite behaviour. The ANNIE approximation works relatively well at high silt contents, with some deviation for more pure clays. On the right hand side of Figure 3 we see the effect of inserting fluid filled cracks, and the ANNIE overburden term is accurate for high clay contents but becomes progressively worse for higher silt

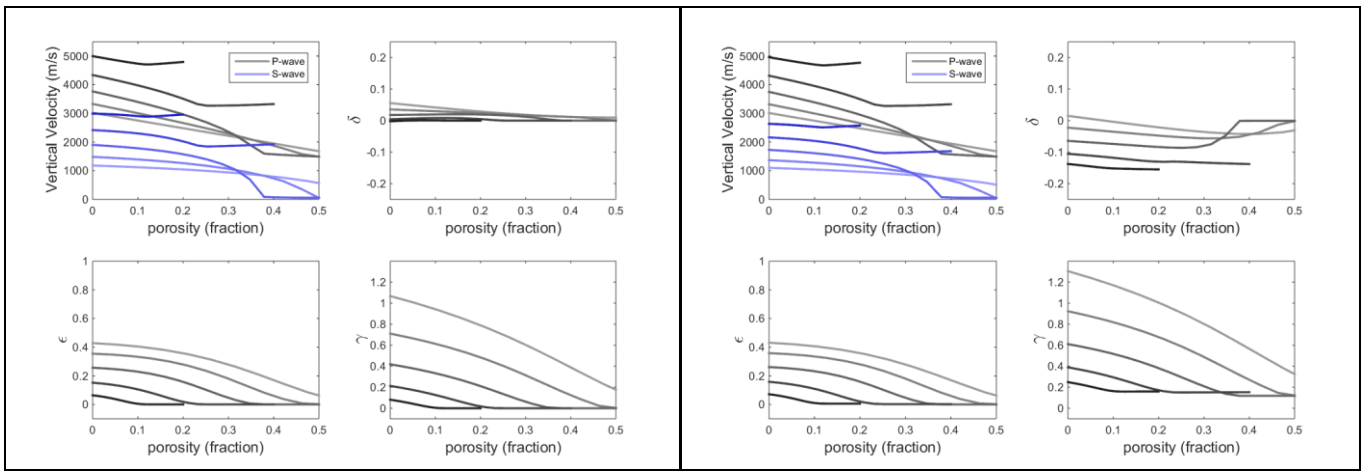

Figure 2: Vertical (bedding perpedicular) velocity and Thomsen parameters for two shales. On the left we have an in-tact shale of varying composition and on the right we have the same shale with horizontal cracks. Contours show increasing silt fraction from zero (lightest) to 0.8 (darkest) in increments of 0.2. All parameters plotted are dynamic.

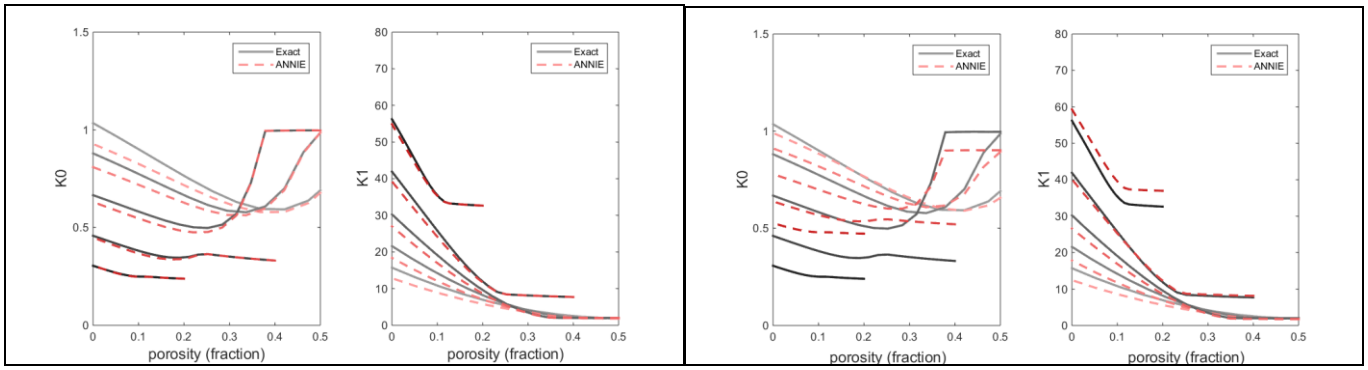

Figure 3: Poroelastic stress coefficients K0 and K1 for in-tact shales (left) and with bedding parallel cracks (right). Contours show increasing silt fraction from zero (lightest) to 0.8 (darkest) in increments of 0.2. Red dashed curves are ANNIE approximations to the exact stress coefficients.

fractions, which makes sense in light of its dependence on δ, which has increased in magnitude. The tectonic term appears correct at for silt fractions of ~60%, but shows some mismatch for higher or lower concentrations. What is also surprising is that the introduction of the saturated cracks hasn't changed the stress coefficients very much at all, as the grey lines on the left and right of Figure 3 are similar. However, our estimates of them have become skewed by the impact of the cracks on velocities and anisotropy, causing the ANNIE mismatch. The ANNIE approximation deteriorates further for the case of dry cracks where δ is large and positive (not shown), a situation not expected in caprock shales but perhaps more applicable to shale gas reservoirs.

Conclusions

The calculation of horizontal stress in an anisotropic medium appears well served by the ANNIE approximation for in-tact shales, but the overburden term K_0 is overestimated when bedding perpendicular cracks are present. This points to the need for characterization of horizontal cracks when present and an improved anisotropic approximation to accurately estimate stresses in shales. These results are contingent on the accuracy of the shale model of Ortega et. al. (2009), which predicts relatively small values for δ, leading to the accuracy of the ANNIE approximation when cracks are not present.

Acknowledgements

I would like to thank Jeremy Meyer from Ikon Science AP for many helpful geomechanical discussions.

References

Collins, P.M., 2002, Injection pressures for geomechanical enhancement of recovery processes in the Athabasca oil sands: Paper SPE 146776 presented at the 2002SPE International Thermal Operations and Heavy Oil Symposium and International Horizontal Well Technology Conference, Calgary, Alberta, November 4-7.

Chesnokov, E., Bayuk, I.O., and Ammerman, M., 2010, Determination of shale stiffness tensor from standard logs: Geophysical Prospecting , 58, 1063-1082.

Haug, K.M., Greene, P. and Mei, S. (2014): Geological characterization of the Lower Clearwater Shale in the Athabasca Oil Sands Area, Townships 87-99, Ranges 1-13, West of Fourth Meridian; Alberta Energy Regulator, AER/AGS Open File Report 2014-04, 33p.

Higgins, S., Goodwin,, S., Donald, A., Bratton, T. and Tracy, G. 2008. Anisotropic stress models improve completion design in the Baxter shale. Paper SPE 115736 presented at the 2008 SPE Annual Technical Conference and Exhibition, Denver, Colorado, 21-24 September.

Holt, R.M., Fjaer, E. and Bauer, A., 2013, Static and dynamic moduli - so equal and yet so different: ARMA 13-521, 7pp.

Hornby, B.E., Schwartz, L.M. and Hudson, J.A. 1994, Anisotropic effective medium modeling of the elastic properties of shales: Geophysics, 59, no.10, 1570-1583.

Jakobsen, M., Hudson, J.A. and Johansen, T.A., 2003, T-matrix approach to shale acoustics: Geophys.J.Int., 154,533-558.

Nishizawa, O., 1982, Seismic velocity in a medium containing oriented cracks- transversely isotropic case: J. Phys. Earth, 30, 331-347.

Katahara, K., 2009, Lateral earth stress and strain: SEG Expanded Abstracts, 2165-2169.

Ortega, J. A., Ulm, F. and Abousleiman, Y., 2009, The nanogranular acoustic signature of shale. Geophysics, 74, no. 3, D65–D84.

Pervukhina, M., Gologoniuc, P., Gurevich, B., Clennell, M.B., Dewhurst, D.N. and Nordgard-Bolas, H.M., 2015, Prediction of sonic velocities in shale from porosity and clay fraction obtained from logs- A North Sea well case study: Geophysics, 80, no.1, D1-D10.

Ren, Q., and Spikes, K., 2014, Anisotropic rock-physics modelling for the Haynesville shale: SEG Expanded Abstracts, 2947-2951.

Sayers, C.M., 2010, The effect of anisotropy on the Young's moduli and Poisson's ratio of shales: SEG Expanded Abstracts, 2606-2610.

Schoenberg, M., Muir, F. and Sayers, C.M., 1996, Introducing ANNIE: A simple three-parameter anisotropic velocity model for shales: J. Seis. Expl., 5, 35-49.

Smith, R. J., Bacon, R. M., Boone, T. J., & Kry, P. R., 2001, Cyclic steam stimulation below a known hydraulically induced shale fracture: JCPT. 43(02).

Thiercelin, M.J., and Plumb, R.A. 1994, Core-based prediction of lithologic stress contrasts in East Texas formations: SPE Formation Evaluation, December 1994, 251-258.

Thomsen, L., 1986, Weak elastic anisotropy, Geophysics, 51, no.10, 1954-1966.

Vernik, L., and Liu, X., 1997, Velocity anisotropy in shales: A petrophysical study: Geophysics, 62, no.2, 521-532.

Waters, G.A., Lewis, R.E. and Bentley, D.C., 2011, The effect of mechanical properties anisotropy in the generation of hydraulic fractures in organic shales: Paper SPE 146776 presented at the 2011 Annual Technical Conference and Exhibition, Denver, Colorado, October 30-November 2.

Xu, S. and Payne, M.A., 2009, Modelling elastic properties in carbonate rocks: The Leading Edge, 66-74.

.